Detection and Quantification of Chloramphenicol in Milk and Honey Using Molecularly Imprinted Polymers: Canadian Penny-Based SERS Nano-Biosensor

Fang Gao, Shaolong Feng, Zhiwen Chen, Eunice C.Y. Li-Chan, Edward Grant, and Xiaonan Lu

Abstract: We integrated molecularly imprinted polymers with surface-enhanced Raman spectroscopy (MIPs-SERS) to develop an innovative nano-biosensor for the determination of chloramphenicol (CAP) in milk and honey products. Template molecule (CAP), functional monomer (acrylamide), cross-linking agent (ethylene glycol dimethacrylate), initiator (2,2'-azobis(isobutyronitrile)), and porogen (methanol) were employed to form MIPs via "dummy" precipitation polymerization. Static and kinetic studies validated the specific selectivity of MIPs toward CAP over nonimprinted polymers (imprinting factor >4). Canadian penny-based silver nano-structure was synthesized as SERS-active substrate for determination of CAP in food matrices. Collected spectra were processed by principal component analysis to differentiate various concentrations of CAP in foods. Partial least squares regression models showed good prediction values ($R > 0.9$) of actual spiked contents (0, 0.1, 0.5, 1, 5 ppm) of CAP in milk and honey. This developed nano-biosensor is low cost, requires little sample pretreatment, and can provide reliable detection of trace level of chemical hazards in food systems within a total of 15 min.

Keywords: biosensor, chloramphenicol, food chemical hazard, molecularly imprinted polymers, SERS

Practical application: Rapid detection of chloramphenicol residues in milk and honey products.

Introduction

Chloramphenicol (CAP) is a broad-spectrum antibiotic originally produced by the bacterium *Streptomyces venezuelae* and used to treat a variety of bacterial infections in humans. However, use of CAP may induce aplastic anemia and bone marrow suppression due to its toxic effect (Vivekanandan and others 2005). Drug abuse is the main factor that causes CAP residues in foods. Many countries, such as China, Canada, United States, and European Union, have strictly banned the use of CAP in food-producing animals (Shi and others 2007). Current methods applied to detect CAP in foods are microbiological test (Singer and Katz 1985), sensors (Ferguson and others 2005), chromatographic methods (for example, gas chromatography-mass spectrometry (Posyniak and others 2003), Liquid chromatography–mass spectrometry (Mottier and others 2003)), and immunoassays (Impens and others 2003). Unfortunately, a few technical challenges exist for these methods. Specifically, laborious sample pretreatment is required due to the interference from food matrices and high-throughput detection of a large amount of samples cannot be realized. Solid phase extraction (SPE) is commonly used as a clean-up method to isolate CAP from food matrices but with unsatisfied selectivity.

MS 20141266 Submitted 7/22/2014, Accepted 10/2/2014. *Authors Gao, Feng, Li-Chan and Lu are with Food, Nutrition and Health Program, Faculty of Land and Food Systems, The Univ. of British Columbia, Vancouver, British Columbia, V6T 1Z4, Canada. Authors Chen and Grant are with Dept. of Chemistry, The Univ. of British Columbia, British Columbia, V6T 1Z1, Canada. Authors Gao is also with Dept. of Chemistry, The Univ. of British Columbia, British Columbia, V6T 1Z1, Canada. Direct inquiries to author Lu (E-mail: xiaonan.lu@ubc.ca).*

Molecularly imprinted polymers (MIPs) have been reported as a unique material to selectively recognize, separate, and enrich different chemical compounds including CAP (Shi and others 2007; Boyd and others 2007). MIPs are recognized as "artificial antibodies" due to their ability to bind specific analytes (Tang and others 2013). In addition, MIPs have the advantages of low cost, ease of preparation, high chemical and thermal stability, and long shelf-life (Mosbach 1994). During the polymerization of MIPs, functional monomers interact with template molecules (for example, CAP) through covalent or noncovalent binding initially, followed by addition of cross-linking agents and initiators; MIPs containing template molecules are thus synthesized. Subsequent removal of the template molecules reveals specific binding sites molded in the MIPs that are completely complementary to the structure of the template molecules and thus able to specifically recognize template molecules with relatively high separation and enrichment efficiency even in a complex matrix such as foods. MIPs have been incorporated as an important element of biosensors for the determination of chemical and microbiological hazards in foods (Lu and others 2010; He and others 2011a). In summary, MIPs can serve as a specific adsorbent for SPE to concentrate target molecules, resulting in lower limit of detection.

Surface-enhanced Raman spectroscopy (SERS) is a rapid, sensitive and nondestructive detection tool to analyze and characterize molecules. This application has overcome the technical barrier of normal Raman spectroscopy, which is the weak intensity of Raman scattering (Lu and others 2011). In SERS, the enhancement of Raman signal may be derived from either electromagnetic (EM) field or chemical effect. Localized surface plasmon resonance

Journal of Food Science A Publication of the Institute of Food Technologists

doi: 10.1111/1750-3841.12705

(LSPR) generated by the incident light is believed to produce an EM field. Molecules adsorbed on or in the proximity to the surface of noble metal (for example, silver and gold) nanostructures would sense the EM field and reradiate the enhanced Raman signal generated by the vibrations of molecules (Craig and others 2013). Sharp surfaces and surface protrusions are most likely to produce enhanced signals with high order due to the probability of generating LSPR, explaining the wide application of roughened metallic surface for SERS. The EM field is the dominant contribution to the enhancement of Raman signal to the orders of 10^6 to 10^8, whereas chemical enhancement is associated with a smaller enhancement effect (approximately 10^2) (Dieringer and others 2006). The total enhancement factor can sometimes reach to 10^{14} to 10^{15} (Xu and others 2000), leading to detection at the single molecule level. This effect has been validated to be feasible by both theoretical calculation based on classic EM theory (Xu and others 2000) and research work for the detection of a single molecule of crystal violet in aqueous colloidal silver solution (Kneipp and others 1997). Recently, researchers have successfully manipulated the detection of single molecule by tip-enhanced Raman spectroscopy (Steidtner and Pettinger 2008) and plasmon-enhanced Raman spectroscopy (Zhang and others 2013) by producing an even stronger EM field for the analyte molecules.

SERS is widely used in the detection of foodborne pathogens (Lu and others 2013), chemical contaminants(He and others 2008; Jackson 2009), and food adulteration (Zhang and others 2010; Shi and others 2014), indicating feasible application in food safety inspection and bioterrorism prevention. A recent work was designed to apply SERS to detect enrofloxacin, furazolidone, and malachite green in fish products after a complicated sample pretreatment (Zhang and others 2012). In another study, SERS was conducted to detect melamine in selective food matrices; only a simple sample pretreatment was required in this case, due to the unique ring breathing mode of triazine in the molecule of melamine, resulting in a unique Raman band at 680 cm^{-1} which could be easily distinguished from Raman bands derived from the remaining food components after sample pretreatment (Shi and others 2014; Lin and others 2008). Because SERS is a detection method and acquires all vibrational modes from existing molecules, in most applications extensive sample pretreatment is required to remove interfering molecules from matrices before detection by SERS and this involves the usage of large amounts of solvents and multiple extraction procedures (for example, liquid–liquid extraction, SPE). To avoid laborious sample pretreatment, other promising separation methods have been proposed to eliminate interferences from matrices before SERS detection. Our group recently developed a microfluidics-based "lab-on-a-chip" system as the separation approach coupled with SERS to detect and differentiate methicillin-sensitive *Staphylococcus aureus* and methicillin-resistant *S. aureus* clinical isolates from China and the United States (Lu and others 2013). This innovative nano-biosensor significantly shortened analysis time and realized high-throughput detection and analysis.

In this study, our objective was to integrate MIPs with SERS to develop a "2-step" nano-biosensor for separation and detection of CAP in different food products, including skim milk, whole milk, and honey. The results demonstrate the potential of MIPs-SRS to serve as an innovative nano-biosensor for rapid, high-throughput, and reliable detection of trace levels of chemical hazards in agricultural and food systems.

Materials and Methods

Chemicals and reagents

Acrylamide (AM; 99% purity), ethylene glycol dimethacrylate (EGDMA; 98% purity), 2,2'-azobis(isobutyronitrile) (AIBN; 99% purity), CAP, silver nitrate, CAP base were purchased from Sigma-Aldrich (St. Louis, MO, USA). Methanol (high-performance liquid chromatography; HPLC grade), acetic acid, sodium chloride, ethyl acetate, and anhydrous sodium sulfate were obtained from Thermo Fisher Scientific (Waltham, MA, USA). Florphenicol was purchased from AK Scientific (Union City, CA, USA). Deionized (DI) water (Millipore (Darmstadt, Germany), 18.2 MΩ/cm) was prepared.

Synthesis of MIPs

CAP (template molecule, 0.5 mmol) was dissolved in 5 mL methanol and then 10 mmol EGDMA (cross-linking agent) and 142 mg AM (monomer) were added. The mixture was sonicated in an ice bath for 5 min, followed by the addition of 20 mg AIBN

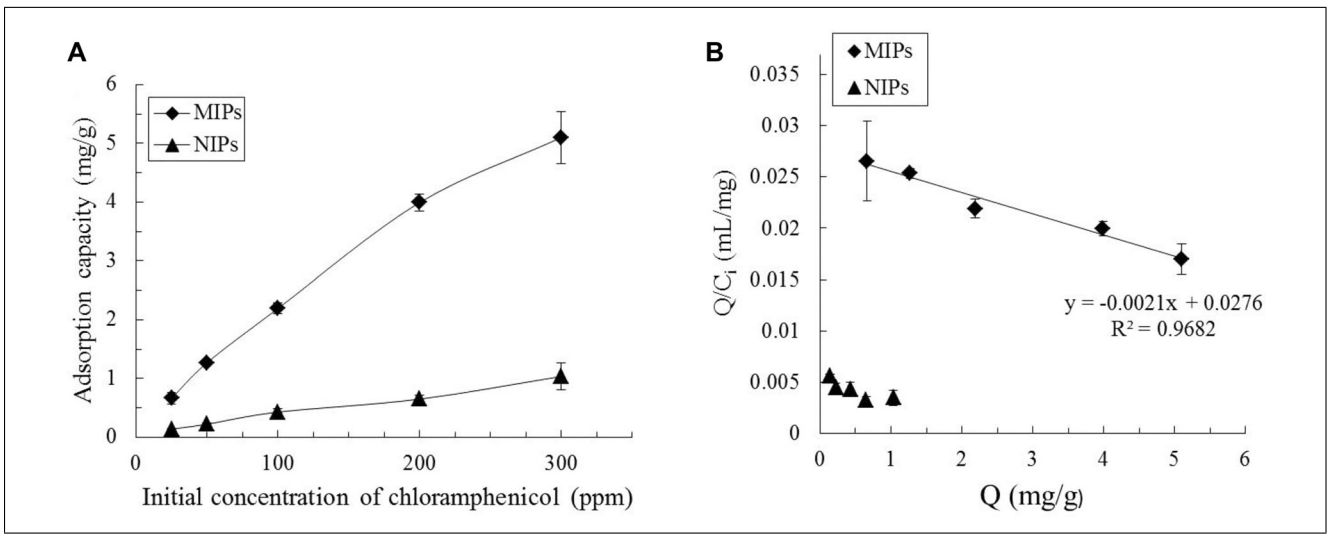

Figure 1–(A) Isotherm of binding properties of molecularly imprinted polymers (MIPs) and nonimprinted polymers (NIPs); (B) Scatchard plot of MIPs and NIPs. Values are shown as mean ± standard deviation ($n = 3$) (initial concentration of CAP in 10% methanol: 25, 50, 100, 200, 300 ppm; time: 3 h).

(initiator). After the solution was purged by nitrogen for another 5 min, polymerization was conducted in an oil bath at 60 °C for 20 h. The formed polymer was sieved through 200-mesh sieve. CAP was removed from the synthesized MIPs by Soxhlet extraction 1st with 300 mL methanol/acetic acid (9:1, v/v) for 24 h, followed by 300 mL methanol until no CAP could be detected based on UV absorbance at 277.5 nm. MIPs were vacuum dried at 22 °C for 4 h. Nonimprinted polymers (NIPs) were also synthesized following the same procedure but with no addition of CAP.

Static and kinetic adsorption capacities of MIPs

To assess the static adsorption capacities, MIPs (20 mg) were added into 2 mL of each of the standard solutions (25, 50, 100, 200, 300 ppm CAP in 10% methanol). The maximum adsorption (λ_{max} = 277.5 nm) was determined by scanning the standard solution from 200 to 800 nm. The calibration curve of absorbance against concentration was also plotted. The mixtures were shaken at 200 rpm for 3 h at 22 °C, and then centrifuged at 13000 × *g* for 20 min. The concentration of CAP in the supernatant was determined by UV absorbance at 277.5 nm. The kinetic adsorption study was carried out by mixing 160 mg MIPs and 16 mL 50 ppm CAP standard solution, followed by shaking at 200 rpm. At different time points (10, 20, 30, 45, 60, 90, 120, 180 min), 1 mL aliquots were taken, centrifuged (13000 × *g*, 20 min), and the concentration of CAP determined by UV absorbance at 277.5 nm. The static and kinetic adsorption capacities of NIPs were determined following the same procedure as described above.

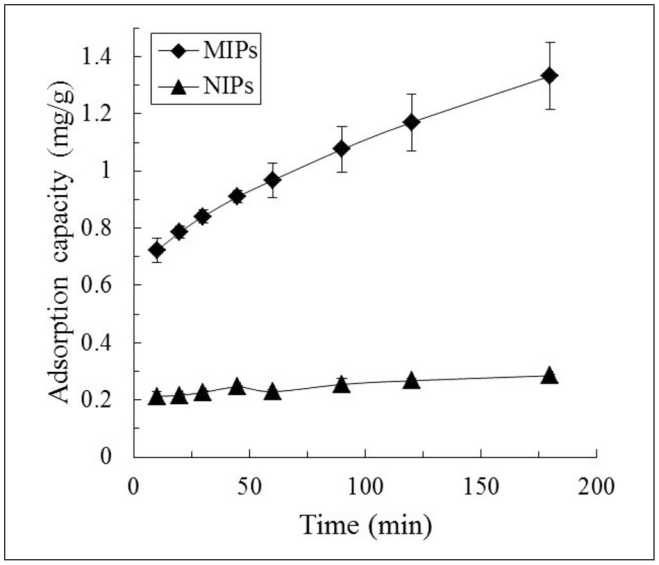

Figure 2–Kinetic study of molecularly imprinted polymers (MIPs) and nonimprinted polymers (NIPs). Values are shown as mean ± standard deviation. (n = 3) (Initial concentration of CAP in 10% methanol: 50 ppm; time points: 10, 20, 30, 45, 60, 90, 120, 180 min).

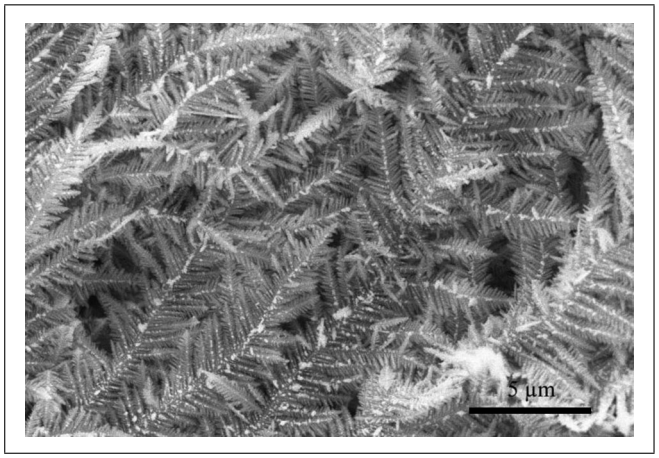

Figure 3–Scanning electron microscope image of silver dendrite formed on Canadian penny.

Interference study was performed by adding 2 mL of florphenicol or CAP base (50 or 300 ppm in 10% methanol aqueous solution) to 20 mg MIPs or NIPs, followed by shaking at 200 rpm for 3 h at 22 °C. The mixture was centrifuged at 13000 × *g* for 20 min and the supernatant was collected and determined by UV spectrometry (224 and 272 nm for florphenicol and CAP base, respectively).

Pretreatment of food samples

Whole milk, skim milk, and honey products were obtained from local grocery stores. Sodium chloride (NaCl, 1 g) was added in 2 mL milk or honey (1 g dissolved in 1 mL DI water), and then spiked with CAP (100 ppm in methanol) for a final concentration of 0, 100 ppb, 500 ppb, 1 ppm, and 5 ppm. Ethyl acetate (5 mL) was then added and the mixture was vortexed for 30 s and centrifuged at 10000 × *g* for 2 min. Top ethyl acetate layer of liquid phase was run through an anhydrous sodium sulfate column to remove water. For milk samples, a 2nd extraction with ethyl acetate was performed, and the 2 extracts were pooled. Dehydrated ethyl acetate was subsequently dried down by rota-vap and finally redissolved in 10% methanol aqueous solution.

Preparation of penny-based silver nano-substrate

The Canadian pre-1996 bronze pennies (98% copper) were selected and sonicated within methanol with 5% acetic acid for 30 min and then washed by methanol (Mabbott and others 2013). Once the penny was dried, 2 µL of 0.1 M silver nitrate solution was deposited onto the surface of penny for 30 s displacement to form silver dendrite spot. Excessive ions were gently washed off with DI water and methanol.

High-performance liquid chromatography

The analyses were conducted on a HPLC system consisting of Agilent 1100 series quaternary pump and a diode array detector. A sample amount of 20 µL (in 50% methanol aqueous solution) was injected on a C_{18} column (µBondapak-C_{18}, 10 µm, 3.9 mm × 300 mm, Waters, Milford, Mass., U.S.A.) and separated by isocratic elution with a mixture of methanol and water (50:50, v/v) at 1.0 mL/min flow rate and 25 °C. The CAP was detected at 278 nm.

Molecularly imprinted SPE (MISPE)

MIPs (100 mg) were packed into a pipette tip (1 mL), which was packed with glass fiber plug at the bottom. A thin layer of sea sand was applied on the top of MIPs. Methanol (3 mL) was 1st added, followed by 3 mL DI water to condition the MISPE. CAP spiked (0, 0.1, 0.5, 1, 5 ppm, respectively) solution (0.2 mL × 5 times) was loaded at 0.33 mL/min, followed by the addition of 1 mL of 15% methanol aqueous solution and 1 mL DI water to wash off interference at 1 mL/min. Finally, CAP was eluted out by 3 mL of 10% acetic acid in methanol solution at 1 mL/min. Flow rate was controlled by the application of vacuum to SPE manifold. The eluents (4 µL) were dried down and redissolved

in 4 μL 50% methanol aqueous solution. The resultant solution was directly deposited onto the silver dendrite spot formed on Canadian penny and blow-dried by nitrogen.

Raman spectroscopy

SERS spectral collection (700 to 1700 cm^{-1}) was conducted using a 785 nm laser (0.25 mW incident laser power) coupled with a 50× objective. The spectrometer (Renishaw, Gloucestershire, UK) has an entrance slit of 50 μm and confocal length of 300 mm and is equipped with a 1200-line/mm grating. Raman scattered light was detected by using a 578 by 385 pixel charge–coupled device array detector. Each spectrum was collected in 10 s. The size of each pixel is 22 μm × 22 μm. Spectra ($N = 8$) from different locations of a sample were collected to study spectral reproducibility.

Chemometric models and statistical analysis

Raman spectra were binned (2 cm^{-1}) and smoothed (9-point Savitzky-Golay algorithm) by using OMNIC version 7.1 (Thermo Electron Corp., Madison, Wis., U.S.A.). Unsupervised principal component analysis (PCA) was conducted to classify samples according to different concentrations of CAP (0, 0.1, 0.5, 1, 5 ppm). Partial least squares regression (PLSR) model was established and cross-validated via "leave-one-out" validation for the quantification and prediction of the actual contents of CAP in milk and honey products. The experiment was performed in at least 3 replicate trials. PCA and PLSR models were established by using Delight version 3.2.1 (D-Squared Development Inc., LaGrande, Oreg., U.S.A.).

Results and Discussion

Evaluation of MIPs performance

"Dummy" precipitation polymerization was carried out using methanol as porogen. The resultant polymer showed uniform and fine powdery form instead of one-piece hard solid synthesized by bulk polymerization, saving tremendous time on grinding and possibly avoiding destroying specific binding sites due to the irregular shape of particles caused by grinding (Mayes and Whitcombe 2005). Parallel polymerization experiment conducted without

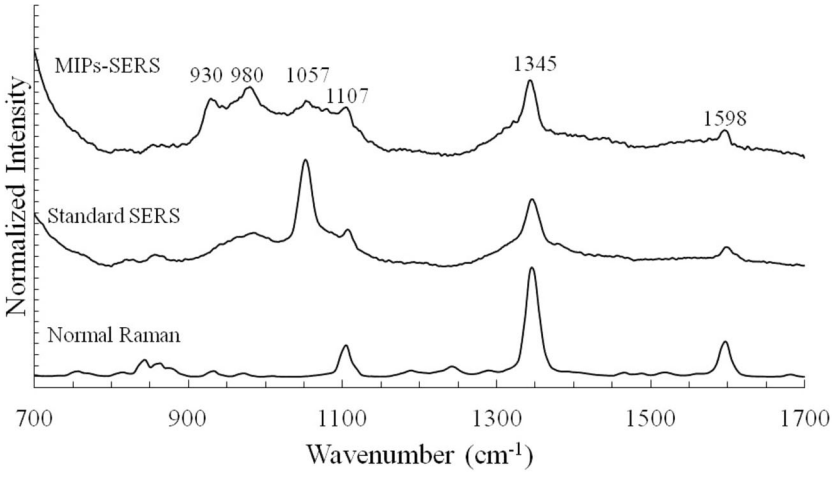

Figure 4–Representative Raman spectra of chloramphenicol (from top to bottom: MIPs-SERS spectrum of extract of CAP-spiked [1 ppm] skim milk, SERS spectrum of standard CAP solution [1 ppm], and normal Raman spectrum of solid crystal). Major band assignments are listed on the top of the spectra.

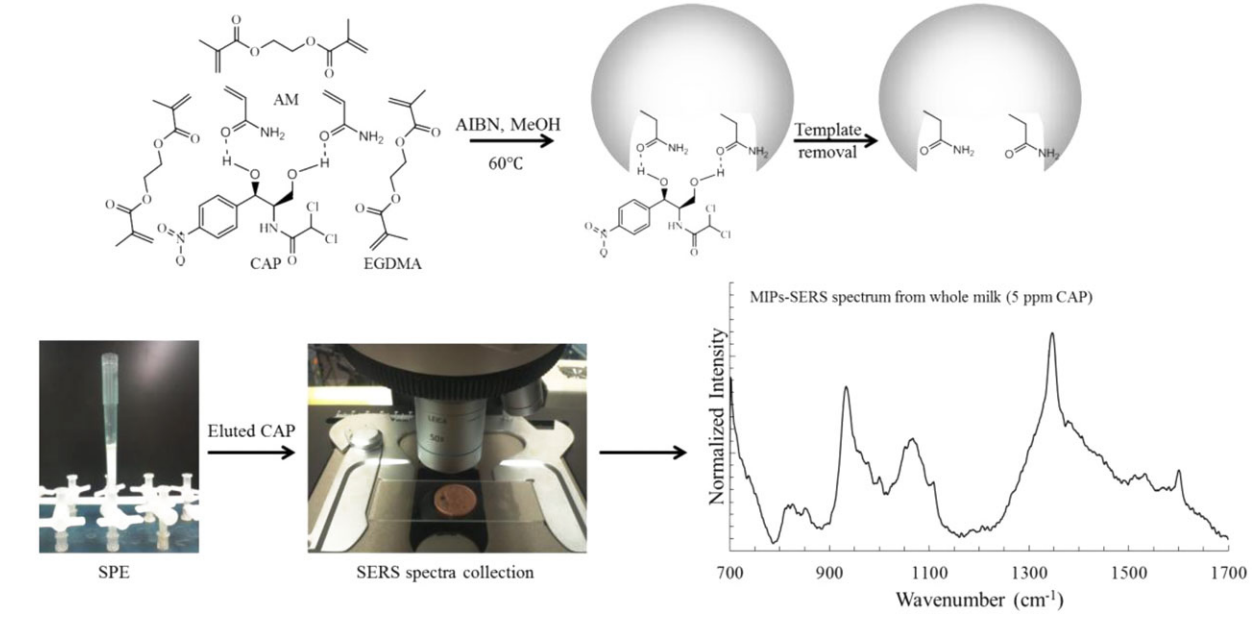

Figure 5–Schematic illustration of the development of MIPs-SERS nano-biosensor to detect chloramphenicol in selective food matrices.

the addition of template molecule and functional monomer validated that methanol tends to break down the cross-linking degree and leads to "dummy" precipitation polymerization without considering large amount of solvent to be used in precipitation polymerization. Size of the fine particle of MIPs may be manipulated by further studies of HPLC packing materials (for example, ratio of methanol to monomers).

Adsorption capacities (Q) of MIPs and NIPs are the major factors that can be used to evaluate the performance of MIPs. Further, imprinting factor (*IF*) is another important factor to assess the selectivity of MIPs over NIPs while Scatchard plot can be used to determine the affinity of MIPs and NIPs (Qian and others 2010). In brief, adsorption capacity is calculated as:

$$Q = (C_i - C_f) \times V / W$$

where C_i is the initial concentration of CAP, C_f represents the final concentration of CAP after polymer adsorption, V is the volume of CAP solution, and W is the amount of the polymers used. *IF* is determined by the equation:

$$IF = Q_{MIPs} / Q_{NIPs}$$

The Scatchard plot is developed according to the equation:

$$Q / C_i = -Q / K_d + Q_{max} / K_d$$

where Q_{max} is the saturated adsorption capacity and K_d is the dissociation constant.

Both static and kinetic studies were carried out using CAP in 10% methanol aqueous solution. Due to improved solubility of CAP in methanol, Q decreased as a function of increasing portion of methanol aqueous solution, in the cases of both MIPs and NIPs (Figure S1). The 10% methanol aqueous solution was selected because this solution provided better IF and an appropriate amount of methanol can further reduce the nonspecific binding caused by low solubility of CAP in aqueous solution.

The binding isotherms of MIPs and NIPs for CAP in the static adsorption studies are shown in Figure 1A. Both Q_{MIPs} and Q_{NIPs} increased as the initial concentration of CAP increased, but the Q_{MIPs} reached 5.10 mg/g while Q_{NIPs} was only 1.05 mg/g at 300 mg/L of the initial CAP solution, leading to an IF value of 4.9 at this concentration. The low adsorption capacity isotherm curve exhibited by NIPs indicate only low level of nonspecific adsorption of NIPs toward CAP; these results also suggest limited nonspecific binding sites in MIPs, indicating that most of the binding sites in MIPs are specific ones. Both the higher Q_{MIPs} isotherm curve and the IF validated that MIPs have much better selectivity toward CAP than NIPs and are suitable for further application of MISPE.

Scatchard analysis showed a linear plot between Q/C_i and Q for MIPs ($R^2 = 0.97$), whereas no linear relationship was observed for NIPs (Figure 1B**)**. The Q_{max} of MIPs calculated according to Scatchard plot was 13.14 mg/g. The linear Scatchard plot of MIPs indicates that the specific binding sites in MIPs are homogenous, which are hypothesized to be driven by hydrogen bonding between MIPs and template molecule (CAP) (Zhu and others 2002). A previous study validated that the strong retention of CAP by MIPs is mainly due to the interaction of 2 hydroxyl groups of CAP and tertiary amine of 2-(diethylamino) ethyl methacrylate (monomer) (Levi and others 1997). For NIPs, we assumed that nonspecific interactions between NIPs and CAP may take place and this nonspecific interaction is mainly associated with hydrophobic interaction (Pan and others 2011).

The results of kinetic adsorption studies are shown in Figure 2. The adsorption capacity of MIPs gradually increased along with time while Q_{NIPs} was almost constant with time. This validated that nonspecific binding is fast but limited, whereas specific binding sites were successfully imprinted in MIPs, resulting in longer times for CAP molecules to orientate themselves to fit into those sites in MIPs.

Interference study was carried out by comparing the adsorption capacity of synthesized MIPs for CAP and 2 CAP structural analogs (that is, florphenicol and CAP base). The adsorption capacity of florphenicol at 50 ppm was 0.66 mg/g for MIPs and 0.10 mg/g for NIPs, respectively. For 300 ppm of florphenicol, the adsorption capacity was 2.70 mg/g for MIPs and 0.81 mg/g for NIPs, respectively. The adsorption capacities of CAP base were 0.03 mg/g for MIPs and 0.02 mg/g for NIPs at 50 ppm, while 1.32 mg/g for MIPs and 0.30 mg/g for NIPs at 300 ppm. Low adsorption capacity of CAP structural analogs indicates the specificity of MIPs toward CAP. The molecular structure of florphenicol is quite similar to CAP, except $-SO_2CH_3$ replaces $-NO_2$ and -F substituents for -OH. CAP base shows no amide tail. Thus, we conclude here both binding and spatial effect contribute to the specific affinity between MIPs and CAP.

The current MIPs were designed and synthesized based upon noncovalent binding, which is easy to process and shows fast rebinding profile. The disadvantage of this type of MIPs is the inevitable nonspecific binding compared to covalent binding-based design. Our developed MIPs significantly decrease the nonspecific binding sites and provide better selectivity of MIPs to template molecules compared to other previous studies (Schirmer and Meisel 2006; Schirmer and Meisel 2009). Previous studies developed MIPs using an analog to CAP as template molecule, which avoids the drawback associated with MIPs of residual template bleeding (Boyd and others 2007). However, the interaction between created MIPs cavities and analyte may be different from template (analyte analog), resulting in less selectivity (IF = 2.43 under HPLC condition (Boyd and others 2007)).

Assessment of MIPs separation of CAP in foods

Honey is a complicated food matrix and therefore extensive sample pretreatment is required to effectively separate and enrich trace level of target molecules in honey and the sample pretreatment generally takes several hours (Kujawski and Namieśnik 2008). Dissolving, hydrolysis, and complicated extraction steps are required to be conducted because honey contains mainly sugars (77% of monosaccharides and oligosaccharides in total) and some other minor components, such as organic acids, proteins, amino acids, and elements (K, P, Mg, Ca, Fe, Si, S, Cu, F, Zn, Mn, Co, Mo, Cr, and I) (Kujawski and Namieśnik 2008). The complex nature of honey poses a technical challenge to separate specific analyte molecules and maintain a decently high level of recovery during sample pretreatment. Milk contains fats, proteins, vitamins, and salts. For separation of target molecules in milk, liquid–liquid extraction is usually performed, followed by basic hydrolysis to break down fats. After neutralization, the solution is concentrated down to a small volume, which is subsequently run through a silica SPE cartridge to further purify the analyte molecules before determination by chromatographic method. The whole process takes about 1 h (Faulkner and others 2000). Taken together, both sample pretreatments involve large amount of organic solvent and are time consuming. Our current sample pretreatment was

performed by minimum operation to initially remove ions, fats, and proteins, saving tremendous amount of time.

MIPs were packed into 1 mL pipette tip used as SPE sorbents (Figure S2). The thin cartridge, slow flow rate (0.33 mL/min) and multiple loading (200 μL × 5) offered CAP a longtime reservation for sufficient interaction with MIPs. Washing with 1 mL of 15% methanol aqueous solution could clean up the polar interferences and may wash the superficially absorbed CAP to the specific binding sites to tightly bind with MIPs, followed by 1 mL water to further remove sugar. Final eluting solvent broke down noncovalent interaction between CAP and MIPs and eluted CAP out. Recoveries of both MISPE and nonimprinted SPE (NISPE) quantified by HPLC are summarized in **Table S1**. NIPs could barely hold CAP even at a low spiked level in foods and showed relatively low recovery (only approximately 20%). In contrast, MIPs show about 2 times recoveries of NIPs, validating the existence of specific binding interaction between MIPs and target molecule (CAP). The relatively low recoveries of MIPs are believed to be due to the slow kinetics of MIPs.

Optimization of process for generating SERS substrate on Canadian penny

Silver dendrite structure has been applied to obtain SERS signals with high enhancement factor and good reproducibility (He and others 2009; Xu and others 2012). This nano-structure is generated by galvanic reaction between reducing metal (for example, zinc) and silver nitrate or silver fluoride solution. By varying the categories of metal as substrate, concentration of silver salts solutions, or reaction time, silver dendrite can be achieved with consistency (Zuo and Jagodzinski 2005; He and others 2009). Gutés and coauthors fabricated a monolayer of silver dendrite produced by galvanic displacement from commercial aluminum foil by depositing it onto double-sided Scotch tape. Excellent SERS results from 1,2-benzenedithiol, 1-phenylethyl mercaptan and 2,2'-dithiodipyridie validated it to be a good candidate as SERS nano-substrate (Gutés and others 2010). In another study, Mabbott and collaborators created a cost-effective method to generate silver dendrite on British 2p coins and demonstrated that it could enhance Raman signals of Rhodamine 6G and 3 drugs, namely 4-methylmethcathinone, 5,6-methylenedioxy-2-aminoindane and 3,4-methylenedioxy-N-methylamphetamine (Mabbott and others 2013).

In this study, silver dendrite was synthesized by depositing silver nitrate solution onto surface-cleaned Canadian penny. Pre-1996 Canadian penny was selected due to its high content of copper (98% purity). A spot of silver dendrite with 3-mm dia was generated by using 2 μL of 1 mol $AgNO_3$. It was found that 30 s of reaction time could produce the dendrite structure that has the best performance for the SERS detection of CAP molecules. Dendritic structure of silver can be clearly observed by scanning electron microscope (Figure 3). Peeling off operation is not required and this leaves the structure intact and uniform. The roughened surface of

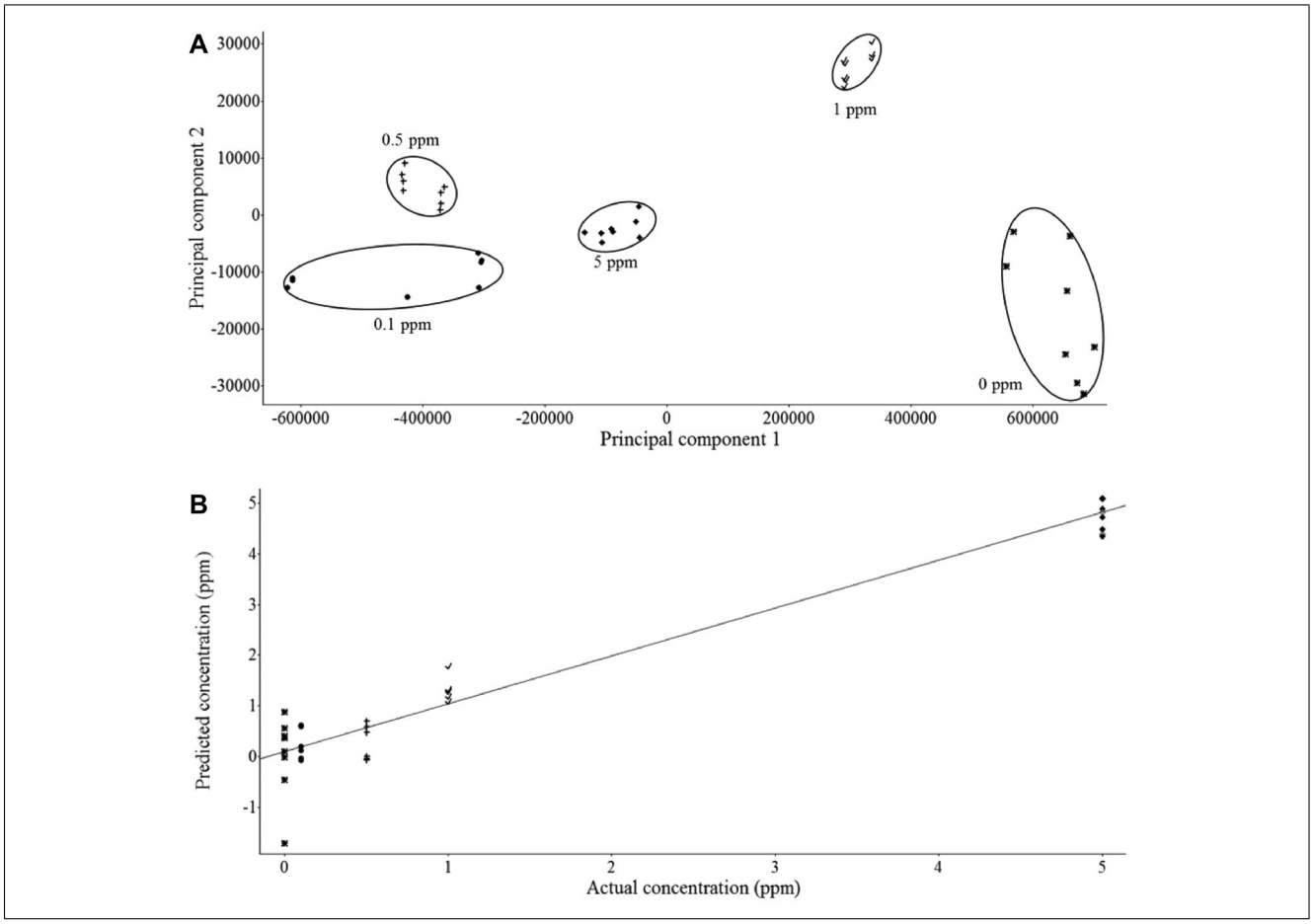

Figure 6–(A) Representative 2-dimensional principal component analysis (PCA) model for differentiation of whole milk containing various concentrations of chloramphenicol (PC1: 95.3%; PC2: 2.1%); (B) representative partial least squares regression (PLSR) model to predict actual concentrations of chloramphenicol in whole milk.

the coin not only provided the substrate for dendritic silver, but also formed a uniform coat tightly adhering to the coin surface to avoid fragmentation, which was reported to occur when depositing onto a bare slide (Lin and others 2004). We blow-dried the solution of CAP spotted on silver dendrite to shorten the drying time and this procedure could also prevent the generation of "coffee ring" (Shen and others 2010) of solution containing target molecule (for example, CAP), which may produce normal Raman signal.

Representative normal Raman spectrum of CAP (solid crystal) in Figure 4 shows 3 major bands at 1107 cm^{-1} (N-H in-plane bending), 1345 cm^{-1} (NO_2 symmetric stretching), and 1598 cm^{-1} (ring stretching) (Lai and others 2011). As comparison, SERS spectrum of standard CAP solution (1 ppm) and MIPs-SERS spectrum of CAP spiked skim milk (1 ppm) are shown on the top of normal Raman spectrum. These 3 prominent peaks assigned to CAP were obviously showing up among samples. Only 2 distinct bands attributed to components from the milk sample after MIPs treatment were found in the MIPs-SERS spectrum; these were at 930 and 980 cm^{-1} (assigned to lactose in skim milk)(Movasaghi and others 2007). The band at 1057 cm^{-1} is assigned to NO_3^- (He and others 2009), which is originated from the synthesis of silver dendrite. Enhanced intensity of Raman bands indicates that CAP anchors itself in its favorite orientation onto the silver dendrite. We believe that silver tends to interact with the electron deficient nitrobenzyl group (Figure S3).

Quantitative analysis of MIPs-SERS nano-biosensor

Figure 5 demonstrates the steps of the synthesis of MIPs and the application of this nano-biosensor integrating MIPs with SERS. In Figure 4, the MIPs-SERS spectrum indicates the capability of cleaning interferences from food matrices by MIPs and provides the enhanced Raman signals of CAP. After spectral collection (700 to 1700 cm^{-1}), chemometric models were constructed to further evaluate the feasibility of MIPs-SERS nano-biosensor. Preprocessed SERS spectra (after bin and smooth) were used to establish unsupervised 2-dimension PCA models. Representative PCA model (Concentrations: 5; Spectra at each concentration: 8) of whole milk is shown in Figure 6A. Different clusters stand for different spiked level of CAP (0, 0.1, 0.5, 1, 5 ppm) in whole milk. Clusters are well segregated, indicating PCA-based Raman spectroscopic analysis could successfully differentiate various CAP contents in whole milk. PCA models of skim milk and honey are shown in Figure S4 and S5, both of which were well established with tight clusters for each spiked concentration. PLSR was applied to the processed SERS spectra and 3 individual PLSR models were established and applied to 3 different food matrices. Figure 6B is the representative PLSR model (Concentrations: 5; Spectra at each concentration: 8) for the quantification of CAP in whole milk. The linearity of the plot ($R = 0.972$) indicates the accurate prediction ability of this PLSR model. In addition, PLSR model of skim milk ($R = 0.975$) (Figure S4 and Table S2) shows a good prediction of the actual concentration of CAP as well. PLSR model of honey provided a less satisfactory quantification and prediction of the actual concentration of CAP ($R = 0.908$) (Figure S5 and Table S2) compared to the ones of whole milk and skim milk. This is probably due to a higher content of sugar residues after MIPs clean-up.

The currently developed MIPs-SERS nano-biosensor could significantly shorten separation and detection time of CAP in food samples without the usage of large amount of solvents. Minimum preextraction of CAP in food samples and further purification of CAP by running MISPE at most take 15 min. Even with MIPs as pretreatment method, common chromatographic measurement takes unavoidable much longer time (at least 10 min for isocratic method) instead of 10 s for individual SERS spectral collection. Therefore, this sensitive and high-throughput MIPs-SERS nano-biosensor is more practicable in the circumstances (for example, in-field and on-line) of monitoring large amount of potentially contaminated agricultural and food samples in a short time period.

Different from chromatographic approach, which provides a 2nd separation by column before detection (Rejtharova and Rejthar 2009), SERS records every probable vibration of molecules including interferences. Therefore, a separation technique is critical for SERS detection. Our group recently integrated MIPs with SERS for the determination of alpha-tocopherol in different vegetable oils (Feng and others 2013). In other studies, aptamer (He and others 2011c) and antibody (He and others 2011b) were introduced as separation method before SERS detection of specific chemical compounds in liquid foods. However, developing specific aptamer is laborious and the commercially available aptamers are still limited. Antibody is sensitive but difficult to be employed for in-field detection because proteins tend to denature under environmental conditions. On the contrary, MIPs are easy to be fabricated, highly selective, and thermal stable, demonstrating to be a good candidate as separation method before SERS detection. Recently, "1-step" MIPs-SERS nano-biosensor has been developed by incorporating silver nanoparticles into MIPs matrices (Liu and others 2011; Xue and others 2013). Generally, 1 h was needed to reach equilibrium of interaction between MIPs-Ag nanoparticles and food samples containing trace level of target analytes.

Conclusions

In conclusion, we developed an innovative MIPs-SERS nano-biosensor, which can rapidly and accurately separate and detect CAP in foods with high throughput capability. MIPs are stable and reusable material to selectively separate CAP from complicated food matrix. Cost-effective Canadian penny can be used to generate silver dendrite as reducing agent. MIPs-SERS nano-biosensor has the potential to determine trace level of chemical hazards in agricultural and food products.

Acknowledgments

We thank Huey Kuan and Benny Chan for technique support and all members in Lu's Food Safety Engineering Laboratory for scientific advice, helpful discussion and critical review of this manuscript. This work was supported by fund awarded to Xiaonan Lu by Natural Sciences and Engineering Research Council of Canada.

References

Boyd B, Bjork H, Billing J, Shimelis O, Axelsson S, Leonora M, Yilmaz E. 2007. Development of an improved method for trace analysis of chloramphenicol using molecularly imprinted polymers. J Chromatogr A 1174:63–71.

Craig AP, Franca AS, Irudayaraj J. 2013. Surface-enhanced Raman spectroscopy applied to food safety. Annu Rev Food Sci Technol 4:369–80.

Dieringer JA, McFarland AD, Shah NC, Stuart DA, Whitney AV, Yonzon CR, Young MA, Zhang X, Van Duyne RP. 2006. Surface enhanced Raman spectroscopy: new materials, concepts, characterization tools, and applications. Faraday Discuss 132:9–26.

Faulkner H, Hussein A, Foran M, Szijarto L. 2000. A survey of vitamin A and D contents of fortified fluid milk in Ontario. J Dairy Sci 83:1210–6.

Feng S, Gao F, Chen Z, Grant E, Kitts DD, Wang S, Lu X. 2013. Determination of α-tocopherol in vegetable oils using a molecularly imprinted polymers-surface-enhanced Raman spectroscopic biosensor. J Agric Food Chem 61:10467–75.

Ferguson J, Baxter A, Young P, Kennedy G, Elliott C, Weigel S, Gatermann R, Ashwin H, Stead S, Sharman M. 2005. Detection of chloramphenicol and chloramphenicol glucuronide

residues in poultry muscle, honey, prawn and milk using a surface plasmon resonance biosensor and Qflex® kit chloramphenicol. Anal Chim Acta 529:109–13.
Gutés A, Carraro C, Maboudian R. 2010. Silver dendrites from galvanic displacement on commercial aluminum foil as an effective SERS substrate. J Am Chem Soc 132:1476–7.
He L, Kim N-J, Li H, Hu Z, Lin M. 2008. Use of a fractal-like gold nanostructure in surface-enhanced Raman spectroscopy for detection of selected food contaminants. J Agric Food Chem 56:9843–7.
He L, Lin M, Li H, Kim N-J. 2009. Surface-enhanced Raman spectroscopy coupled with dendritic silver nanosubstrate for detection of restricted antibiotics. J Raman Spectrosc 41:739–44.
He J, Fang G, Deng Q, Wang S. 2011a. Preparation, characterization and application of organic-inorganic hybrid ractopamine multi-template molecularly imprinted capillary monolithic column. Anal Chim Acta 692:57–62.
He L, Haynes CL, Diez-Gonzalez F, Labuza TP. 2011b. Rapid detection of a foreign protein in milk using IMS-SERS. J Raman Spectrosc 42:1428–34.
He L, Lamont E, Veeregowda B, Sreevatsan S, Haynes CL, Diez-Gonzalez F, Labuza TP. 2011c. Aptamer-based surface-enhanced Raman scattering detection of ricin in liquid foods. Chem Sci 2:1579–82.
Impens S, Reybroeck W, Vercammen J, Courtheyn D, Ooghe S, De Wasch K, Smedts W, De Brabander H. 2003. Screening and confirmation of chloramphenicol in shrimp tissue using ELISA in combination with GC–MS^2 and LC–MS^2. Anal Chim Acta 483:153–63.
Jackson LS. 2009. Chemical food safety issues in the United States: Past, present, and future. J Agric Food Chem 57:8161–70.
Kneipp K, Wang Y, Kneipp H, Perelman LT, Itzkan I, Dasari RR, Feld MS. 1997. Single molecule detection using surface-enhanced Raman scattering (SERS). Phys Rev Lett 78: 1667–1670.
Kujawski MW, Namieśnik J. 2008. Challenges in preparing honey samples for chromatographic determination of contaminants and trace residues. Trends Anal Chem 27:785–93.
Lai K, Zhang Y, Du R, Zhai F, Rasco BA, Huang Y. 2011. Determination of chloramphenicol and crystal violet with surface enhanced Raman spectroscopy. Sens Instrumen Food Qual 5:19–24.
Levi R, McNiven S, Piletsky SA, Cheong S-H, Yano K, Karube I. 1997. Optical detection of chloramphenicol using molecularly imprinted polymers. Anal Chem 69:2017–21.
Lin H, Mock J, Smith D, Gao T, Sailor MJ. 2004. Surface-enhanced Raman scattering from silver-plated porous silicon. J Phys Chem B 108:11654–9.
Lin M, He L, Awika J, Yang L, Ledoux D, Li H, Mustapha A. 2008. Detection of melamine in gluten, chicken feed, and processed foods using surface enhanced Raman spectroscopy and HPLC. J Food Sci 73:T129–34.
Liu P, Liu R, Guan G, Jiang C, Wang S, Zhang Z. 2011. Surface-enhanced Raman scattering sensor for theophylline determination by molecular imprinting on silver nanoparticles. Analyst 136:4152–8.
Lu Q, Chen X, Nie L, Luo J, Jiang H, Chen L, Hu Q, Du S, Zhang Z. 2010. Tuning of the vinyl groups' spacing at surface of modified silica in preparation of high density imprinted layer-coated silica nanoparticles: a dispersive solid-phase extraction materials for chlorpyrifos. Talanta 81:959–66.
Lu X, Al-Qadiri HM, Lin M, Rasco BA. 2011. Application of mid-infrared and Raman spectroscopy to the study of bacteria. Food Bioprocess Technol 4:919–35.
Lu X, Samuelson DR, Xu Y, Zhang H, Wang S, Rasco BA, Xu J, Konkel ME. 2013. Detecting and tracking nosocomial methicillin-resistant *Staphylococcus aureus* using a microfluidic SERS biosensor. Anal Chem 85:2320–7.
Mabbott S, Eckmann A, Casiraghi C, Goodacre R. 2013. 2p or not 2p: tuppence-based SERS for the detection of illicit materials. Analyst 138:118–22.
Mayes AG, Whitcombe MJ. 2005. Synthetic strategies for the generation of molecularly imprinted organic polymers. Adv Drug Deliv Rev 57:1742–78.
Mosbach K. 1994. Molecular imprinting. Trends Biochem Sci 19:9–14.
Mottier P, Parisod V, Gremaud E, Guy P, Stadler R. 2003. Determination of the antibiotic chloramphenicol in meat and seafood products by liquid chromatography–electrospray ionization tandem mass spectrometry. J Chromatogr A 994:75–84.
Movasaghi Z, Rehman S, Rehman IU. 2007. Raman spectroscopy of biological itssues. Appl Spectrosc Rev 42:493–541.
Pan G, Zhang Y, Ma Y, Li C, Zhang H. 2011. Efficient one-pot synthesis of water-compatible molecularly imprinted polymer microspheres by facile RAFT precipitation polymerization. Angew Chem Intl Ed Engl 50:11731–4.
Posyniak A, Zmudzki J, Niedzielska J. 2003. Evaluation of sample preparation for control of chloramphenicol residues in porcine tissues by enzyme-linked immunosorbent assay and liquid chromatography. Anal Chim Acta 483:307–11.
Qian K, Fang G, He J, Pan M, Wang S. 2010. Preparation and application of a molecularly imprinted polymer for the determination of trace metolcarb in food matrices by high performance liquid chromatography. J Sep Sci 33:2079–85.
Rejtharova M, Rejthar L. 2009. Determination of chloramphenicol in urine, feed water, milk and honey samples using molecular imprinted polymer clean-up. J Chromatogr A 1216:8246–53.
Schirmer C, Meisel H. 2006. Synthesis of a molecularly imprinted polymer for the selective solid-phase extraction of chloramphenicol from honey. J Chromatogr A 1132:325–8.
Schirmer C, Meisel H. 2009. Chromatographic evaluation of polymers imprinted with analogs of chloramphenicol and application to selective solid-phase extraction. Anal Bioanal Chem 394:2249–55.
Shen X, Ho C-M, Wong T-S. 2010. Minimal size of coffee ring structure. J Phys Chem B 114:5269–74.
Shi X, Wu A, Zheng S, Li R, Zhang D. 2007. Molecularly imprinted polymer microspheres for solid-phase extraction of chloramphenicol residues in foods. J Chromatogr B Analyt Technol Biomed Life Sci 850:24–30.
Shi Y-e, Li L, Yang M, Jiang X, Zhao Q, Zhan J. 2014. A disordered silver nanowires membrane for extraction and surface-enhanced Raman spectroscopy detection. Analyst 139:2525–30.
Singer CJ, Katz SE. 1985. Microbiological assay for chloramphenicol residues. J Assoc Off Anal Chem 68:1037–41.
Steidtner J, Pettinger B. 2008. Tip-enhanced Raman spectroscopy and microscopy on single dye molecules with 15 nm resolution. Phys Rev Lett 100:236101–1–236101–4.
Tang Y, Fang G, Wang S, Sun J, Qian K. 2013. Rapid determination of metolcarb residues in foods using a biomimetic enzyme-linked immunosorbent assay employing a novel molecularly imprinted polymer film as artificial antibody. J AOAC Intl 96:453–8.
Vivekanandan K, Swamy MG, Prasad S, Mukherjee R. 2005. A simple method of isolation of chloramphenicol in honey and its estimation by liquid chromatography coupled to electrospray ionization tandem mass spectrometry. Rapid Commun Mass Spectrom 19: 3025–30.
Xu H, Aizpurua J, Käll M, Apell P. 2000. Electromagnetic contributions to single-molecule sensitivity in surface-enhanced Raman scattering. Phys Rev E Stat Plasmas Fluids Relat Interdiscip Topics 62:4318–24.
Xu H, Shao M, Chen T, Zhao Y, Lee S-T. 2012. Surface-enhanced Raman scattering on silver dendrite with different growth directions. J Raman Spectrosc 43:396–404.
Xue JQ, Li DW, Qu LL, Long YT. 2013. Surface-imprinted core-shell Au nanoparticles for selective detection of bisphenol A based on surface-enhanced Raman scattering. Anal Chim Acta 777:57–62.
Zhang XF, Zou MQ, Qi XH, Liu F, Zhu XH, Zhao BH. 2010. Detection of melamine in liquid milk using surface-enhanced Raman scattering spectroscopy. J Raman Spectrosc 41: 1655–60.
Zhang Y, Huang Y, Zhai F, Du R, Liu Y, Lai K. 2012. Analyses of enrofloxacin, furazolidone and malachite green in fish products with surface-enhanced Raman spectroscopy. Food Chem 135:845–50.
Zhang R, Zhang Y, Dong ZC, Jiang S, Zhang C, Chen LG, Zhang L, Liao Y, Aizpurua J, Luo Y, Yang JL, Hou JG. 2013. Chemical mapping of a single molecule by plasmon-enhanced Raman scattering. Nature 498:82–6.
Zhu Q-Z, Haupt K, Knopp D, Niessner R. 2002. Molecularly imprinted polymer for metsulfuron-methyl and its binding characteristics for sulfonylurea herbicides. Anal Chim Acta 468:217–27.
Zuo C, Jagodzinski PW. 2005. Surface-enhanced Raman scattering of pyridine using different metals: differences and explanation based on the selective formation of α-pyridyl on metal surfaces. J Phys Chem B 109:1788–93.

Supporting Information

Disclaimer: Supplementary materials have been peer-reviewed but not copyedited.

Figure S1. Adsorption capacity of molecularly imprinted polymers (MIPs) and nonimprinted polymers (NIPs) according to the change of methanol portion in aqueous solution (initial concentration of CAP: 50 ppm; time: 3 h).

Figure S2. Illustration of molecularly imprinted solid phase extraction (MISPE) for chloramphenicol.

Figure S3. Schematic model of orientation of chloramphenicol on silver dendrite.

Figure S4. (A) Representative 2-dimensional principal component analysis (PCA) model for separation of skim milk containing different concentrations of chloramphenicol (PC1: 93.8%; PC2: 2.8%); (B) representative partial least squares regression (PLSR) model to predict actual concentrations of chloramphenicol in skim milk.

Figure S5. (A) Representative 2-dimensional principal component analysis (PCA) model for separation of honey containing different concentrations of chloramphenicol (PC1: 73.3%; PC2: 9.5%); (B) representative partial least squares regression (PLSR) model to predict actual concentrations of chloramphenicol in honey.

Figure S6. (A) Chemical structure of florphenicol; (B) chemical structure of chloramphenicol base.

Table S1. Spiked recoveries molecularly imprinted solid phase extraction (MISPE) and nonimprinted solid phase extraction (NISPE).

Table S2. Partial least squares regression (PLSR) models for the prediction of chloramphenicol concentration in foods.